Project 2
MUSCL reconstruction

Paride Passelli and Niko Masiero

Numerical methods for conservation laws
Swiss Federal Institute of Technology in Lausanne

Prof. J.S. Hesthaven

December 30, 2018

The objective of this project is to apply the MUSCL reconstruction. For this purpose, as in Project1, we consider the one-dimensional *shallow water* equation:

$$\begin{bmatrix} h \\ m \end{bmatrix}_{tt} + \begin{bmatrix} m \\ \frac{m^2}{h} + \frac{1}{2}gh^2 \end{bmatrix}_x = \mathbf{S}(x,t)$$

Where we define $h = h(x,t)$, $m = m(x,t)$, we set the acceleration due to gravity $g = 1$. $\mathbf{S}$ is a source term, we define also the horizontal velocity $u = \frac{m}{h}$ and the spatial domain $\Omega = [0,2]$.
We define $\mathbf{q} = [h,m]^T$, hence the previous equation can be rewritten as follows:

$$\mathbf{q}_t + f(\mathbf{q})_x = \mathbf{S}(x,t), \tag{1}$$

where

$$f(\mathbf{q}) = \begin{bmatrix} m \\ \frac{m^2}{h} + \frac{1}{2}gh^2 \end{bmatrix}$$

Hence we can redefine (1) as follow:

$$\mathbf{q}_t + \nabla_{\mathbf{q}} f(\mathbf{q})_x = \mathbf{S}(x,t) \tag{2}$$

After computation of the Jacobian

$$\nabla_{\mathbf{q}} f = \begin{bmatrix} 0 & 1 \\ -\frac{m^2}{h^2} + gh & \frac{2m}{h} \end{bmatrix}$$

we obtain

$$\begin{bmatrix} h \\ m \end{bmatrix}_t + \begin{bmatrix} 0 & 1 \\ -\frac{m^2}{h^2} + gh & \frac{2m}{h} \end{bmatrix} \begin{bmatrix} h \\ m \end{bmatrix}_x = \mathbf{S}(x,t)$$

The objective is to obtain an high-order accurate scheme, for this purpose we consider the semi-discrete finite volume scheme, that as suggested, is obtained after integration of the conservation law in each cell $I_i = [x_{i-\frac{1}{2}}, x_{i+\frac{1}{2}}]$.

$$\frac{dq_i}{dt} = -\frac{1}{h}(F_{i+\frac{1}{2}} - F_{i-\frac{1}{2}}) + S_i(t) \tag{3}$$

where q_i and S_i are cell averages and $F_{1\pm\frac{1}{2}}$ is a consistent numerical flux approximating $f(q_{i\pm\frac{1}{2}})$. We need to keep in mind that we want high spatial accuracy, but also high temporal accuracy. To achieve the first objective we can apply the MUSCL approach, while for the second purpose we will apply the third order SSP-RK3.

1 MUSCL

We briefly recall the MUSCL algorithm. Suppose we want to solve the following general conservation law

$$u_t + f(u)_x = 0$$

Step 1 $u_j^{n+\frac{1}{2}} {}_j^n - \frac{k}{2h} f'(\bar{u_j})\delta u_j$
Step 2 $u_{j\mp\frac{1}{2}}^{n+\frac{1}{2},\pm} = u_j^{n+\frac{1}{2}} \mp \delta\frac{u_j}{2}$
Step 3 $u_j^{n+1} = u_j^n - \frac{k}{h}(F(u_{j+\frac{1}{2}}^{n+\frac{1}{2},-}, u_{j+\frac{1}{2}}^{n+\frac{1}{2},+}) - F(u_{j-\frac{1}{2}}^{n+\frac{1}{2},-}, u_{j-\frac{1}{2}}^{n+\frac{1}{2},+}))$
This can be easily generalized to our case.

2 SSP-RK3

We describe here the SSP-Rk3 algorithm, it consists in a time-marching strategy to solve the system in equation (3). Suppose we want to solve the following ODE

$$\frac{dq_i}{dt} = L(q,t)$$

then given q^n we can compute q^{n+1} as follows:
$q^{(1)} = q^{(n)} + kL(q^n, t^n)$
$q^{(2)} = \frac{3}{4}q^{(n)} + \frac{1}{4}(q^{(1)} + kL(q^{(1)}, t^n + k))$
$q^{(3)} = \frac{1}{3}q^{(n)} + \frac{2}{3}(q^{(2)} + kL(q^{(2)}, t^n + \frac{k}{2}))$
$q^{n+1} = q^{(3)}$

3 Lax-Friedrichs implementation

For details on the Lax-Friedrichs flux you can refer to project 1. We implement the MUSCL scheme for the one-dimensional shallow water equation. We use the Lax-Friedrichs flux (for more details on Lax-Friedrichs flux see Projet 1). We apply SSP-RK3 in order to update the solution. This choice would avoid the use of characteristic variables in the integration step (more complicate). Moreover we evaluate the slopes for the MUSCL scheme using different slopes:

- Zero slope
- Minmod limiter
- MUSCL limiter
- Minmod TVB limiter (with parameter M)...

We discretize the mesh in N elements and $N+1$ points, we tested the code in different cases implying boundary conditions, initial conditions and also different source terms. In the following sections we use the notation $\mathbf{u}_i = \frac{m(x_i,t)}{h(x_i,t)}$ defining the ratio between the two quantities that we need to compute.

3.1 First case

We start by testing our code with the following initial conditions:

$$h(x,0) = 1 + \frac{1}{2}sin(\pi x)$$

$$m(x,0) = uh(x,0)$$

and periodic boundary conditions $q_0 = q_{N-1}$ and $q_N = q_1$ Moreover we impose the following source

$$S(x,t) = \begin{bmatrix} \frac{\pi}{2}(u-1)cos(\pi(x-t)) \\ \frac{\pi}{2}cos(\pi(x-t))(-u+u^2+gh(x-t,0)) \end{bmatrix}$$

and we evaluate the time-step as

$$k = \text{CFL}\frac{\Delta x}{\max_i(|u_i| + \sqrt{gh_i})}$$

with CFL$= \frac{1}{2}$ and $T = 2$.
Zero slope
We can observe the plot of the solution against the true solution at final time $T = 2$ for two different number of grid points (Figure 1 using zero slope. We observe that there is some problem in the m. This is consistent since we choose a zero slope and the solution in reflected. This problem get less evident if we refine the grid (but still present). In

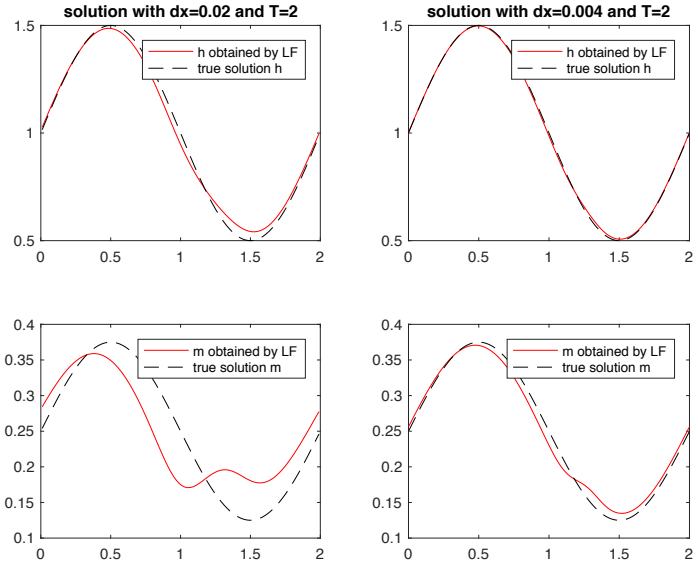

Figure 1: Numerical solution with zero slope

Figure 2 we can observe the error of the scheme at $T = 2$ as a function of Δx.

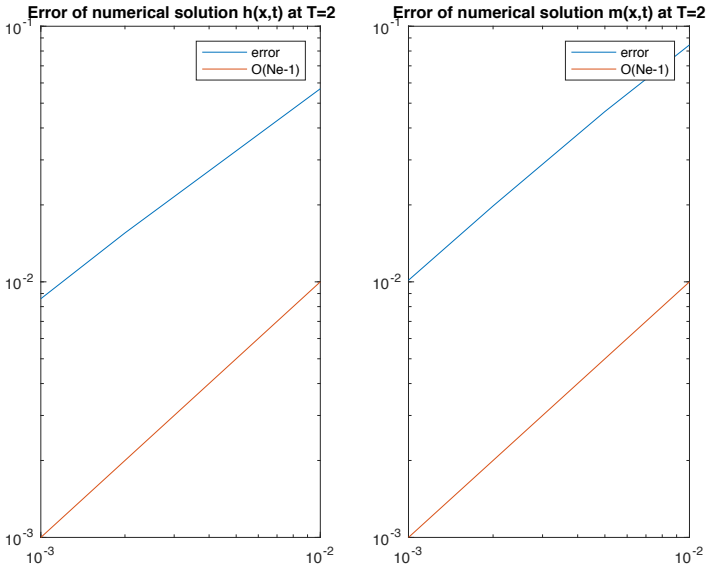

Figure 2: Numerical error with zero slope

Minmod limiter

In Figure 3 we can observe the numerical solution against the true solution for different number of grid points. We can observe a clear improvement respect the previous case. We also plot the error of the scheme at T=2 as a function of Δx on a log-log graph. We

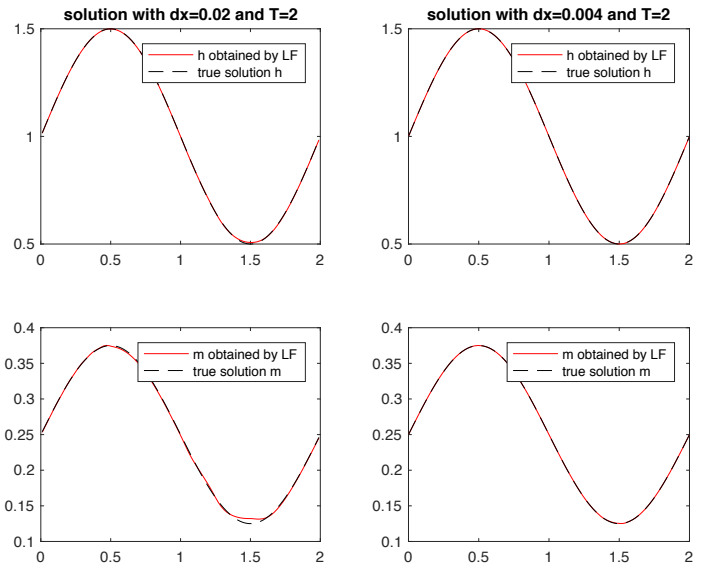

Figure 3: Numerical solution with minmod limiter

observe the order of convergence is 2 as expected (Figure 4).

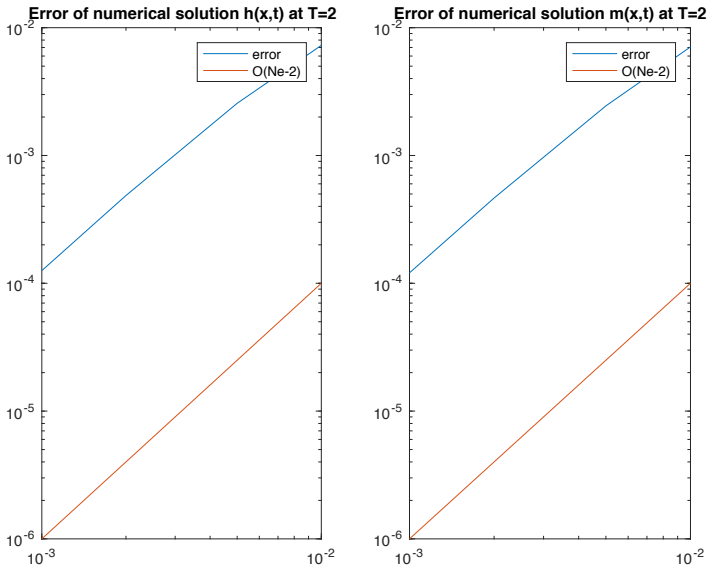

Figure 4: Numerical error with minmod limiter

MUSCL limiter
This time we use the MUSCL limiter and we test again our code. We can observe the numerical solution at final time against the true one in Figure 5. There is also this time an improvement with respect to the previous case. As always we can plot also the measure of the error of this scheme. We expect an order of convergence (with respect to Δx) of 2. This is the case (Figure 6).
MinmodTVB limiter
This time we repeat the experiment taking the minmod-type TVB limiter with parameter M. We have to choose the right M. The idea of minmod-type TVB is to address the problem of reduction of accuracy around local extreme. The bigger the M is the more we expect accuracy at the smooth extreme improves. We need, anyway, to keep in mind that we must pay attention to this choice. In fact to high choices of M can reintroduce oscillations. We try to choose the best M by trial and error. These tests can be observed in Figure 7.
It seems that a reasonable choice is $M = 32$. Notice that since the initial conditions are smooth in this case taking a bigger value of M doesn't reintroduce oscillations, this will no more be the case for the other initial conditions we have to test. We then plot the numerical solution against the true one with this choice. The resulting plot can be find in Figure 8.

We can also plot the error once more to see a clear result (Figure 9. In any case the order of convergence in space in 2 as expected.

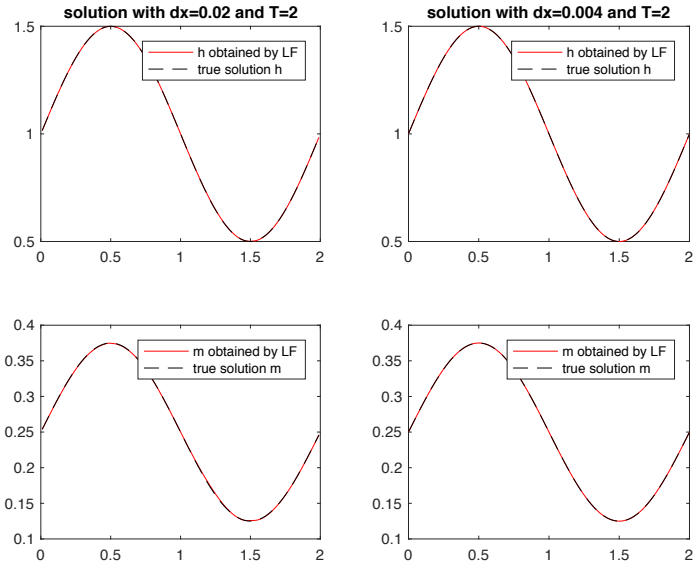

Figure 5: Numerical solution with muscl limiter

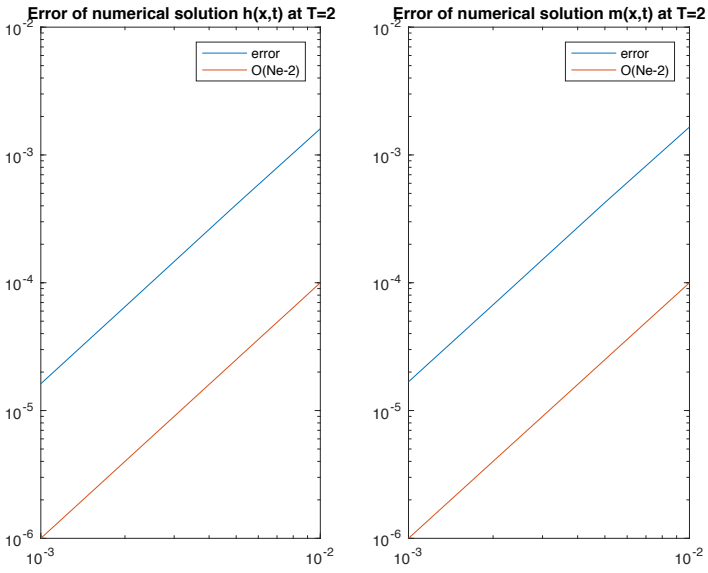

Figure 6: Numerical solution with muscl limiter

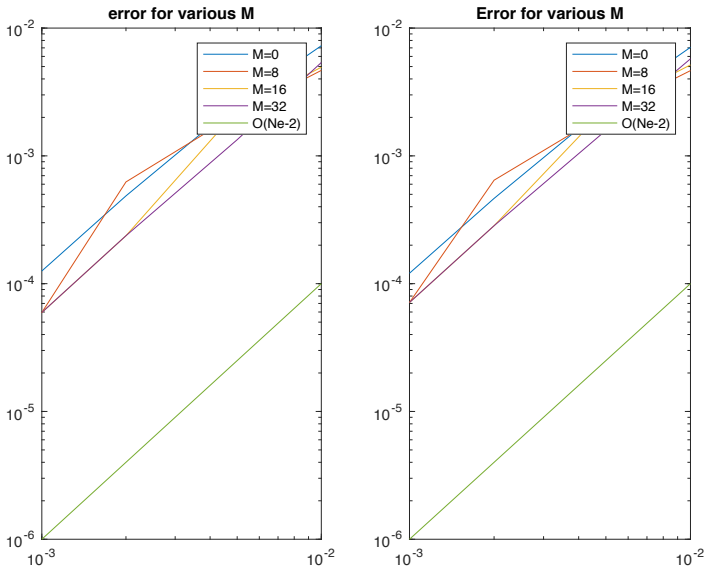

Figure 7: Numerical error for different M for MinmodTVB limiter

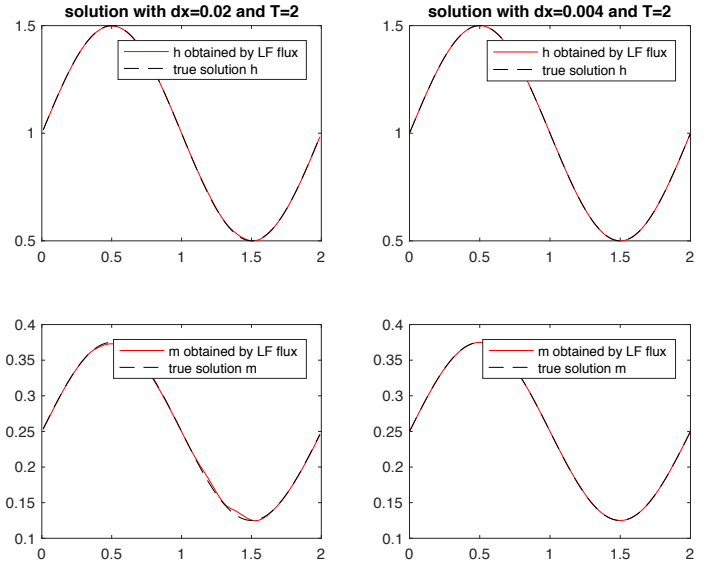

Figure 8: Numerical solution for M=32 for MinmodTVB limiter

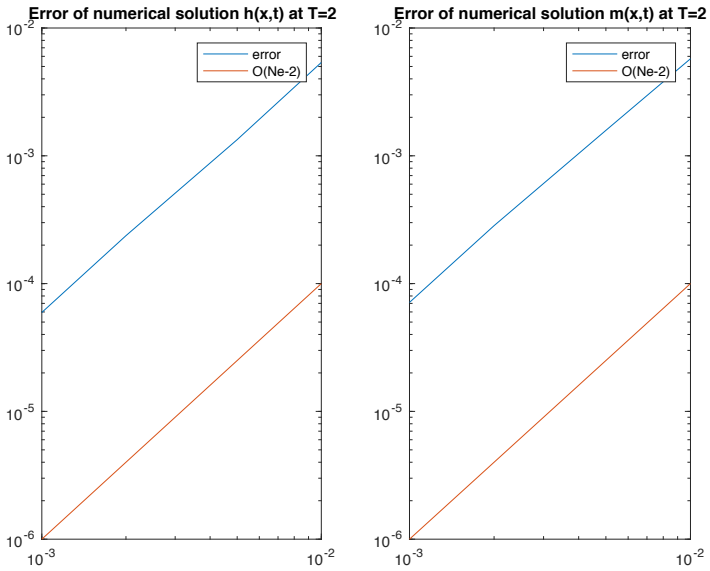

Figure 9: Numerical error for M=32 for MinmodTVB limiter

We can observe a plot of the numerical solutions (with all type of slope together) for different values of grid points against the true solution.

3.2 second case

Now we run again our matlab program with the following initial conditions: $h(x,0) = 1 - 0.1sin(\pi x)$, $m(x,0) = 0$ and source term equal to zero. We take periodic boundary conditions. As always we analyze the four limiter separately and at the end we observe the global result. As reference solution we compute once a solution with the MUSCL limiter on a very fine mesh ($\Delta x = 0.0005$).

Zero slope

We observe the numerical solution at final time $T = 2$ against the reference one for two different number of point grids (Figure 10).

We plot also the error as function of Δx and we observe that the order of convergence is 1 (Figure 11).

Minmod limiter

We run the experiment with the Minmod limiter. In Figure 12 we can see the numerical solution against the true solution (the reference one).

The plot of the error at final time as function of Δx can be find in Figure 13. As expected the error decay is 2.

MUSCL limiter

In Figure 14 we find the numerical solution with muscl limiter against the reference one at final time.

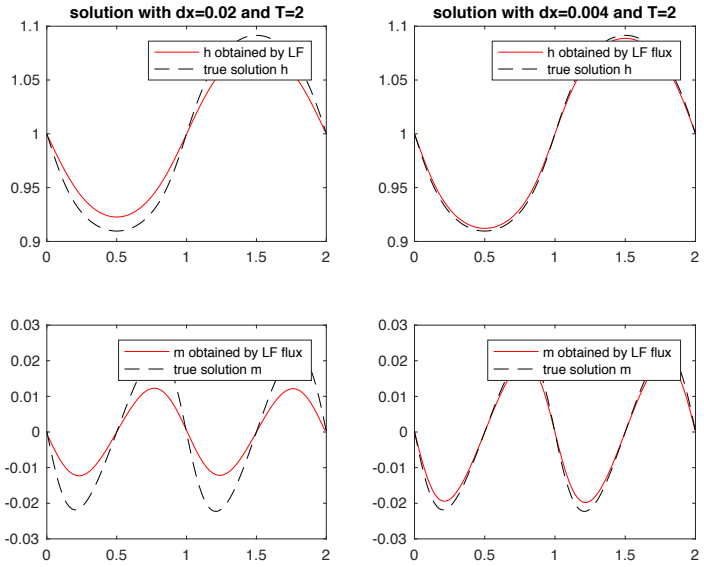

Figure 10: Numerical solution with zero slope

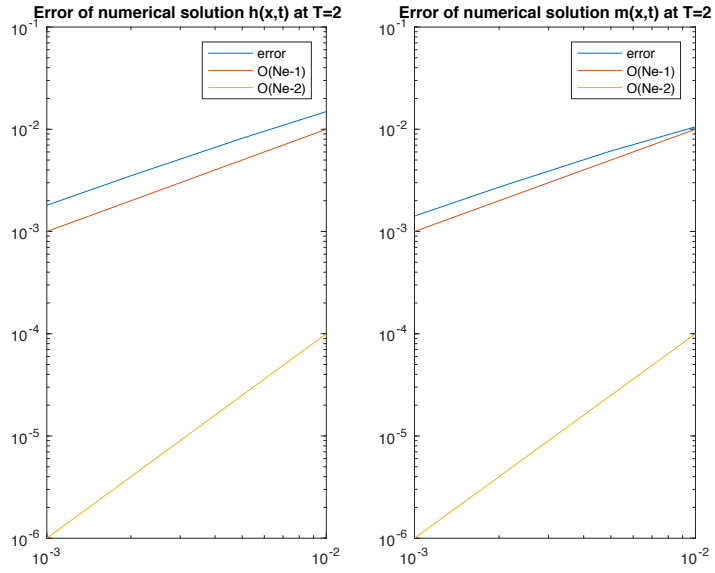

Figure 11: Numerical error with zero slope

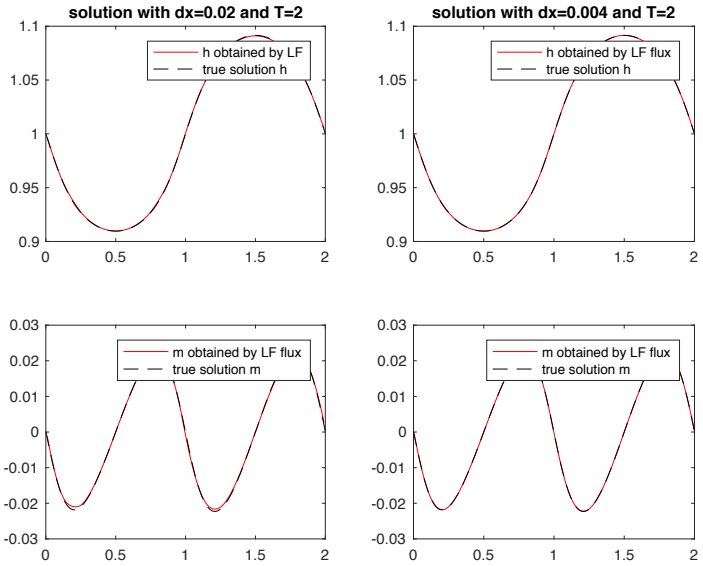

Figure 12: Numerical solution with minmod limiter

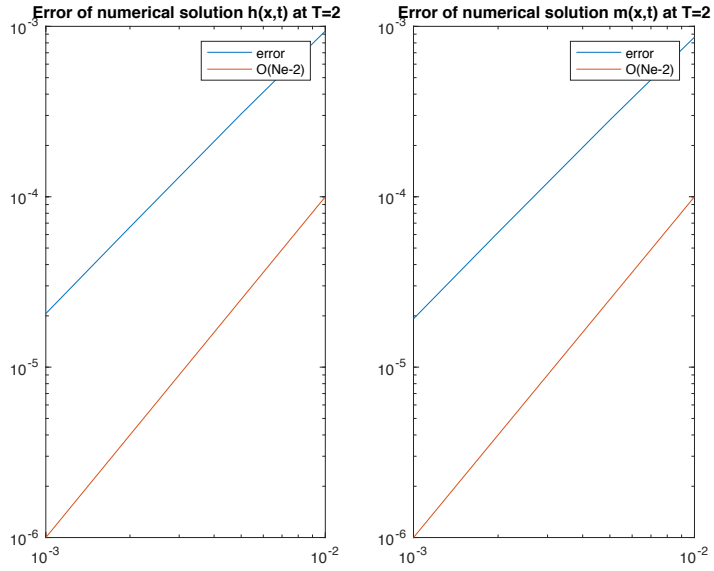

Figure 13: Numerical error with minmod limiter

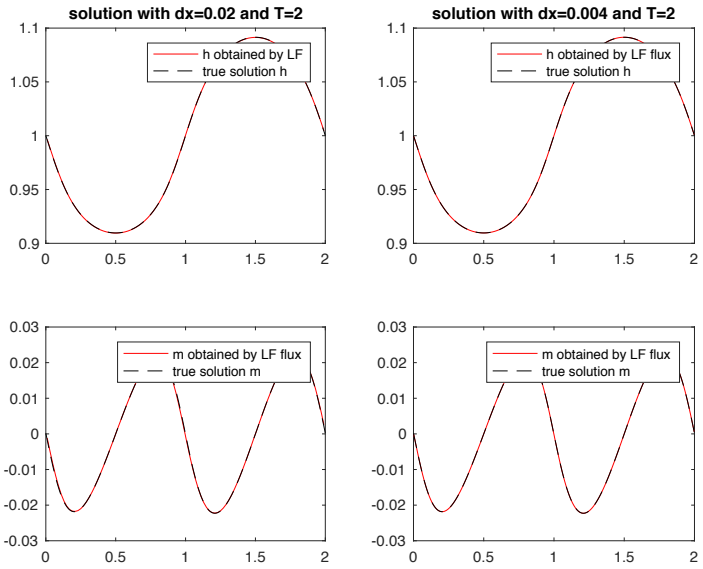

Figure 14: Numerical solution with muscl limiter

As always we also plot the error in a log-log graph and we observe an order of convergence in space of 2 (Figure 15).

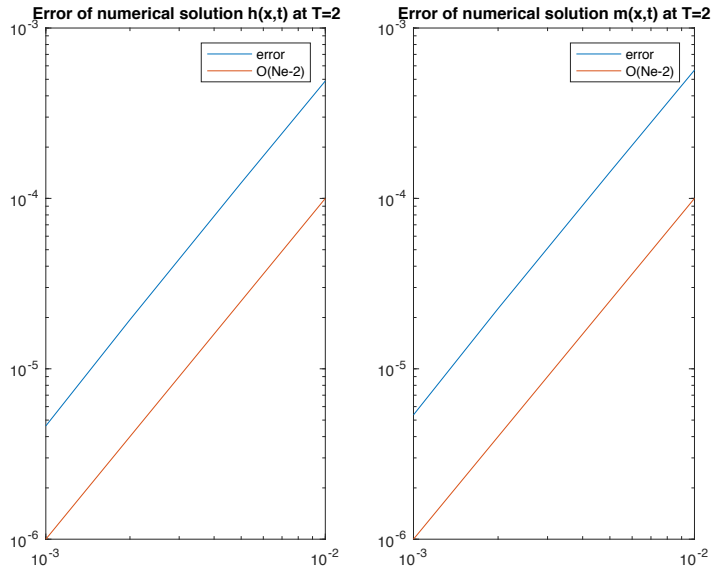

Figure 15: Numerical solution with muscl limiter

Minmod-type TVB limiter

As before we need to discuss the choice of M. We try some possible choice and look for the smaller M that achieve the maximal accuracy for the smooth part. Figure 16 suggest that a good choice of $M = 80$. In this plot we observe the error for different M of h (left) and m (right).

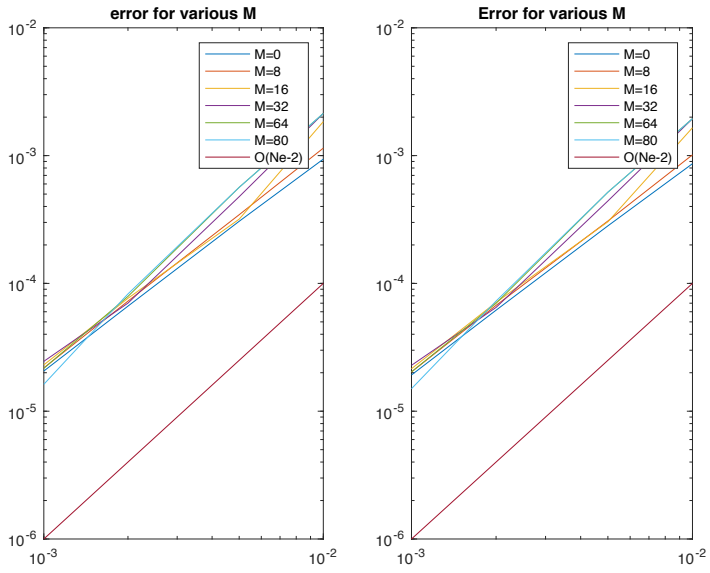

Figure 16: Numerical errors for different M with minmod-tvb limiter

Thus with this choice of M we plot the numerical solution at final time against the reference one (Figure17).
We observe the error in Figure 18.
Notice that in this case M is different from the previous case.

3.3 third case

Last, we repeat for the last time the simulation using the usual method for different slope using the previous setting, but with initial conditions:

$$h(x, 0) = 1 - 0.2sin(2\pi x)$$

and

$$m(x, 0) = 0.5$$

As in the previous case we compute a reference solution with MUSCL limiter on a fine grid (Δx=0.005).
Zero slope
In Figure 19 we observe the numerical solution against the reference one at final time $T = 2$. The precision of the solution is in general better with more grid points but the fact that the true solution is not differentiable give some issue.

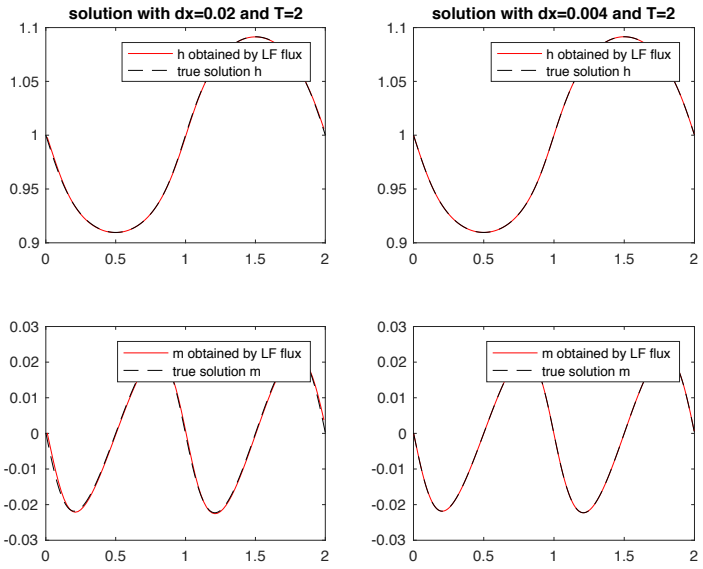

Figure 17: Numerical solution with $M = 80$ minmod-tvb limiter

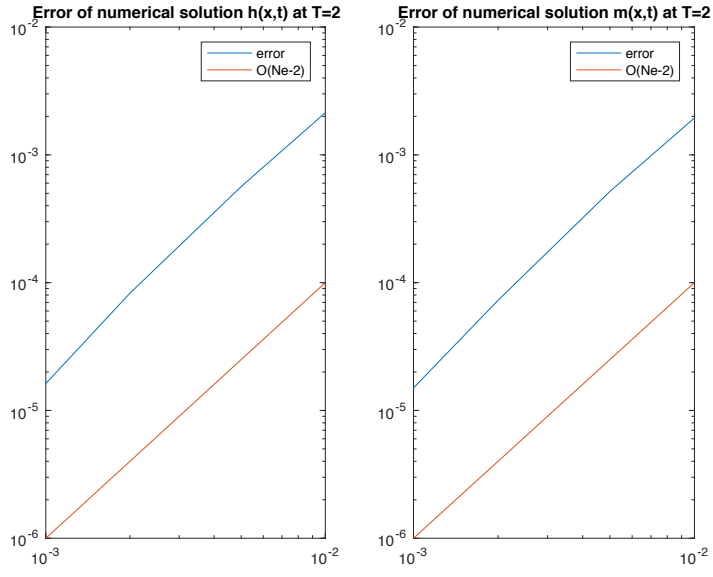

Figure 18: Numerical error with M=80 for minmod-tvb limiter

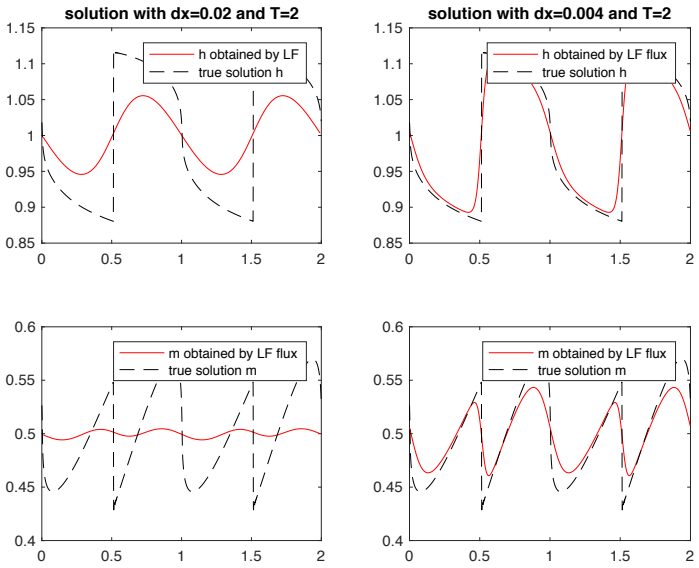

Figure 19: Numerical solution with zero slope

In figure 20 we can see that the maximal error has not a convergence of order 1, because of the non differentiability.

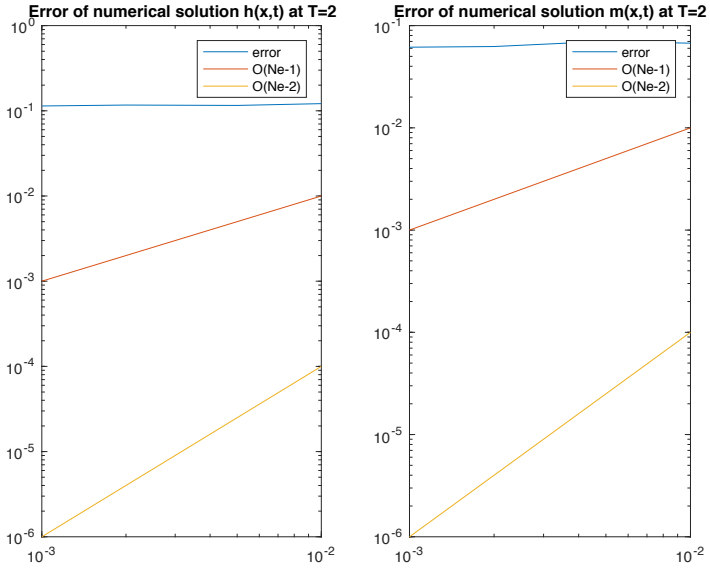

Figure 20: Numerical error with zero slope

Minmod limiter

We can observe in Figure 21 that this time the numerical solution approximate better the reference one (in particular with the finest grid).

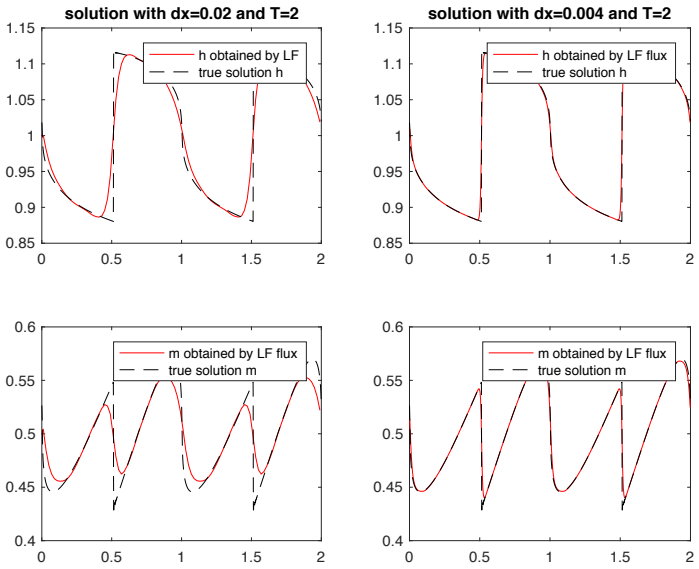

Figure 21: Numerical solution with minmod limiter

In figure 22, as before, we can see that the maximal error has not a convergence of order 2, because of the non differentiability.
MUSCL limiter
In Figure 23 we observe that the numerical solution is always better.
As in the previous case, being not differentiable, the error at final time doesn't have convergence order 2 (Figure 24).
Minmod-type TVB limiter
As before we try to find a good value of M. This time the generla error analysis is not possible, since the solution is not derivable. Instead we just look with some trials the maximal M that doesn't reintroduce any oscillations. We choose $M = 10$, the numerical solution can be observed in Figure 25.
We can also observe the numerical solution with $M = 60$ in Figure 26. Here we observe the reintroduction of the oscillations that we wanted to avoid.
This time we have chosen a smaller M in order to avoid oscillations, so we have lost in accuracy.

4 Roe flux implementation

We repeat all the test done with the Lax-Friedrich flux also for the Roe flux. As for the Lax-Friedrich flux, the theory can be find in the previous project We use, as always, a discretization of the mesh in N elements and $N + 1$ points. As in the previous section

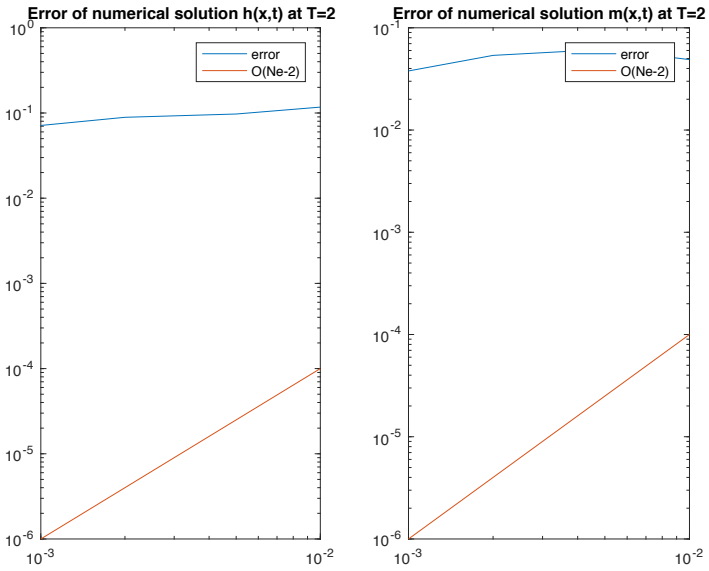

Figure 22: Numerical error with zero slope

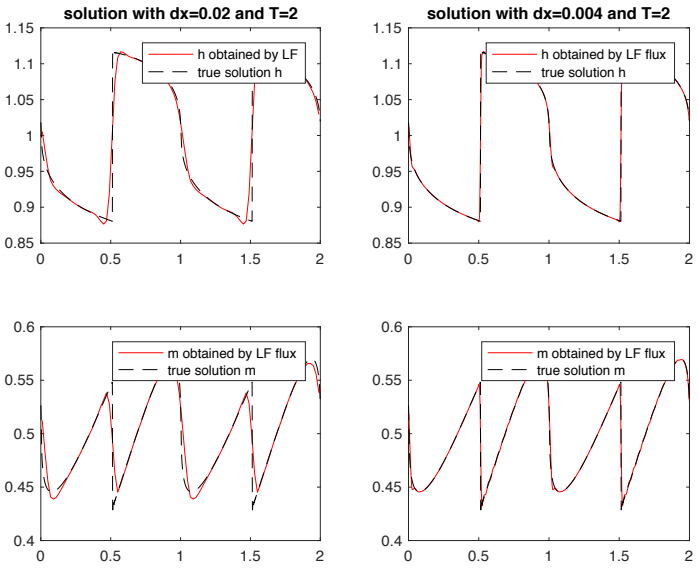

Figure 23: Numerical solution with muscl limiter

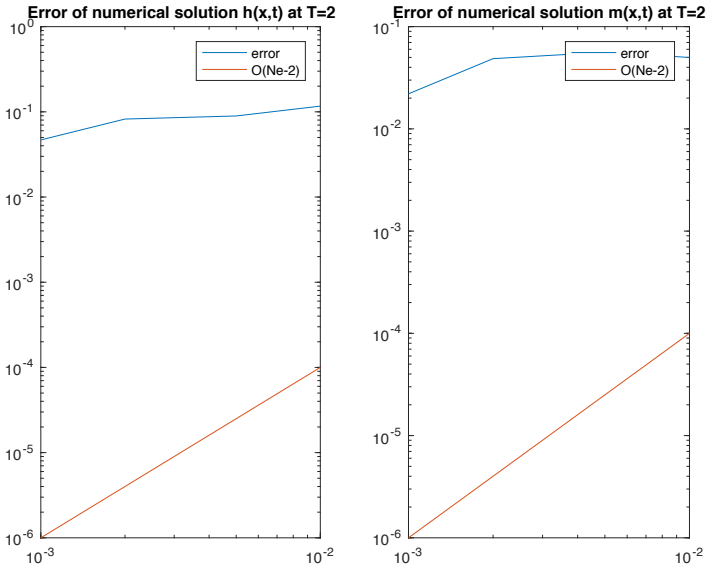

Figure 24: Numerical error with muscl limiter

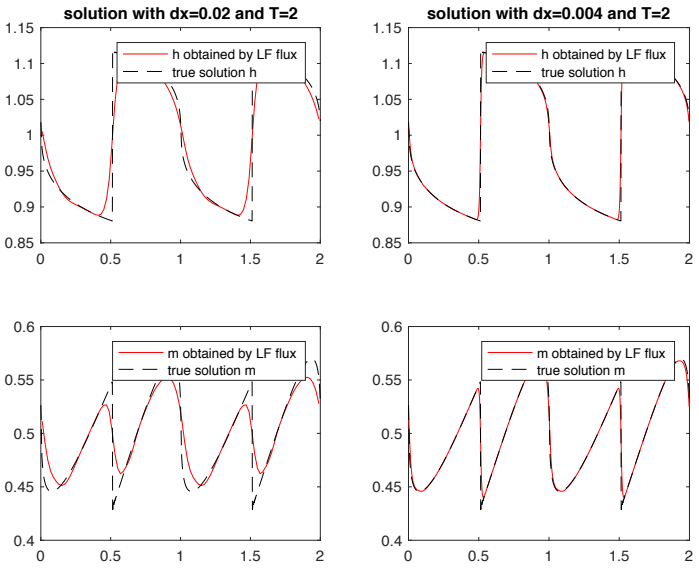

Figure 25: Numerical solution with minmod-tvb limiter and M=10

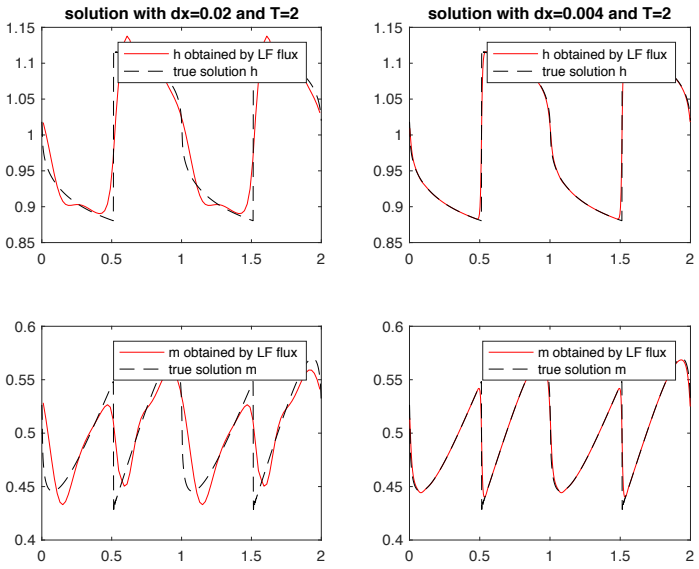

Figure 26: Numerical solution with minmod-tvb limiter and M=60

we test the MUSCL scheme for different slopes.

4.1 First case

We test our code, as in subsection 2.1, with the following initial conditions:

$$h(x,0) = 1 + \frac{1}{2}sin(\pi x)$$

$$m(x,0) = uh(x,0)$$

and periodic boundary conditions $q_0 = q_{N-1}$ and $q_N = q_1$ Moreover we impose the following source

$$S(x,t) = \begin{bmatrix} \frac{\pi}{2}(u-1)cos(\pi(x-t)) \\ \frac{\pi}{2}cos(\pi(x-t))(-u+u^2+gh(x-t,0)) \end{bmatrix}$$

and we evaluate the time-step as

$$k = \text{CFL}\frac{\Delta x}{\max_i(|u_i| + \sqrt{gh_i})}$$

with CFL$= \frac{1}{2}$ and $T = 2$.
Zero slope
We test the method with the Roe flux using zero slope. We can observe the numerical solution at final time against the true one in Figure 27

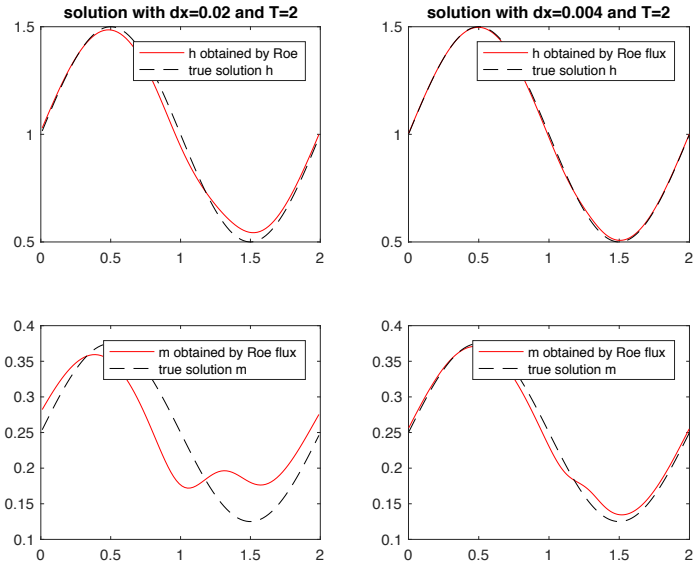

Figure 27: Numerical solution with zero slope

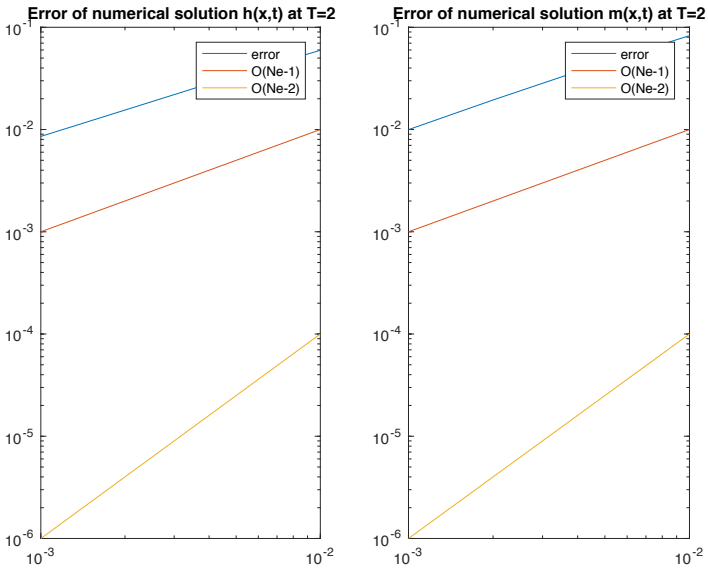

Figure 28: Numerical error with zero slope

As usual we also plot the error of the scheme at $T = 2$ as function of Δx on a log-log graph. In Figure 28 we observe a convergence of order 1 in space.

Minmod limiter

We repeat the experiment with the Minmod limiter. We observe a better behaviour at final time of the numerical solution with respect to the previous case (Figure 29).

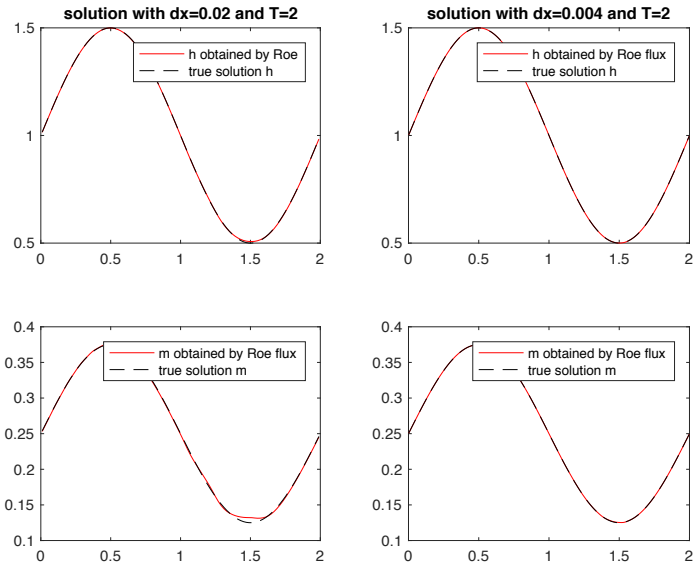

Figure 29: Numerical solution with minmod limiter

We also observe that the rate of convergence in space is 2 (Figure 30).

MUSCL limiter With this slope choice we have better results (Figure 31) We can observe that the numerical solution approximate always better the true one (already with 500 grid points). Once more the error convergence (as function of Δx) is equal to 2 (Figure 32).

Minmod-type TVB limiter

As in the Lax-Friedrich case we need to choose a good M in order to avoid the reduction of the accuracy and to avoid the reintroduction of oscillations. As before there is no problem in high M since the solution is smooth so we choose the smaller M that approximately give accuracy 2. In this case $M = 64$ (Figure 33).

Moreover in Figure 34 we can observe the error with $M = 64$ and in Figure 35 the plot of the numerical solution at final time.

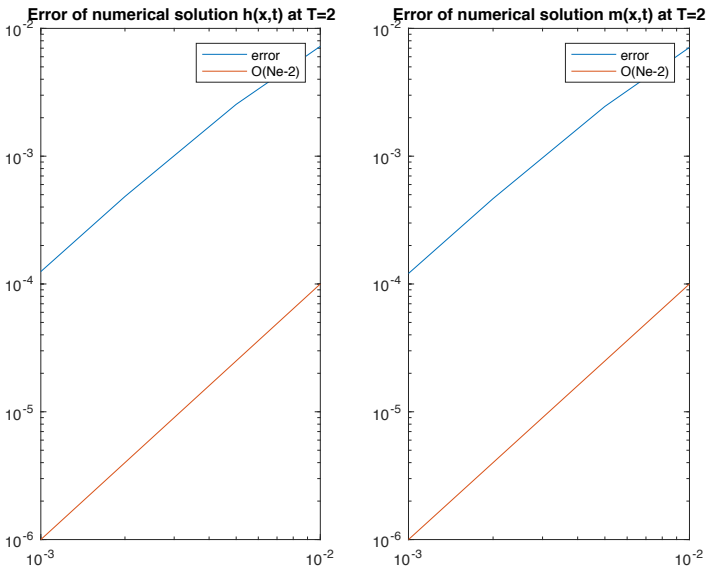

Figure 30: Numerical error with minmod limiter

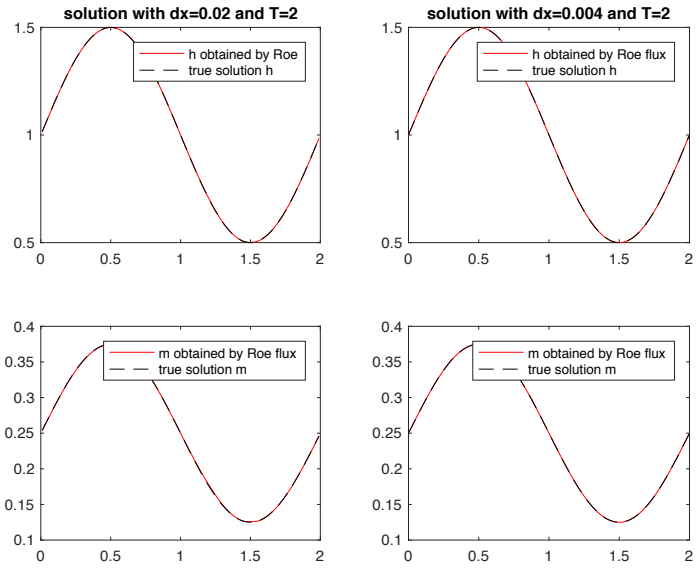

Figure 31: Numerical solution with muscl limiter

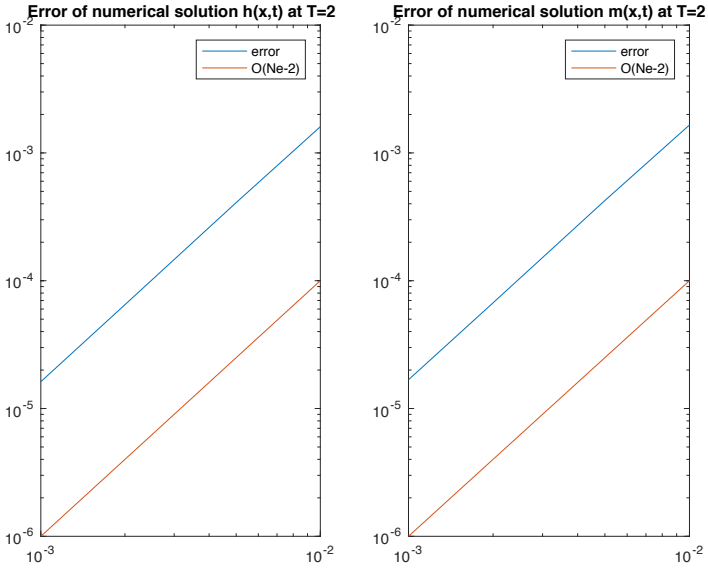

Figure 32: Numerical error with muscl limiter

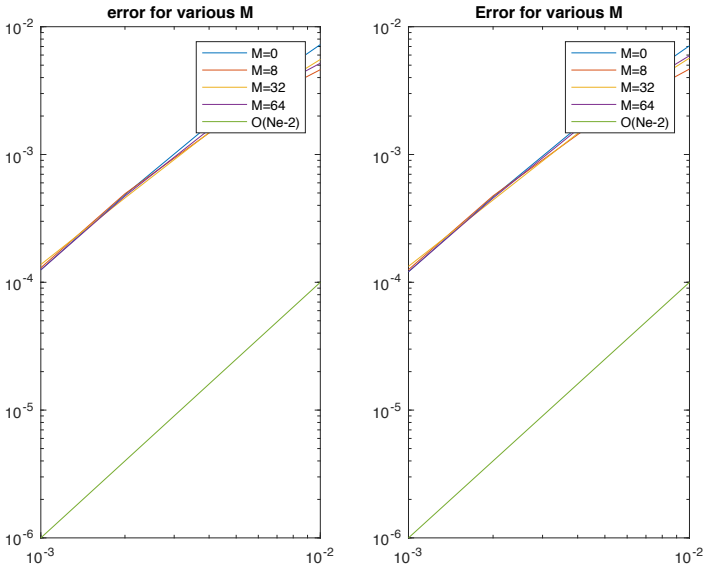

Figure 33: Numerical error with minmod-type tvb limiter for different M

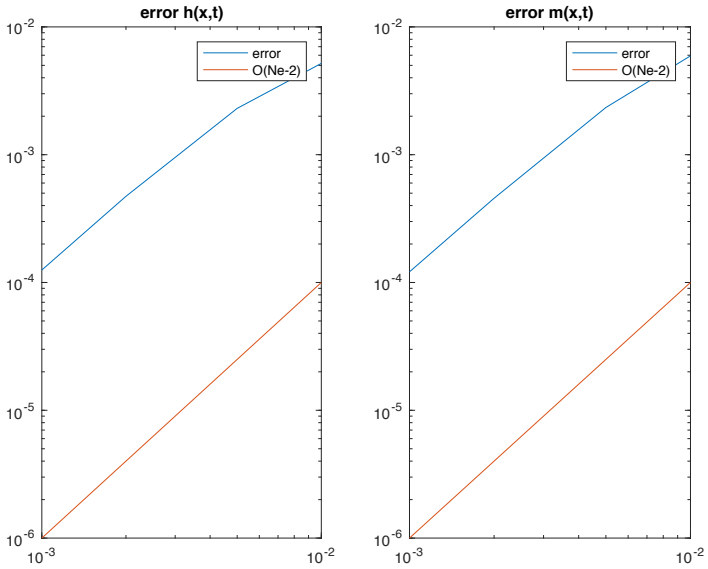

Figure 34: Numerical error with minmod-type tvb limiter for different M

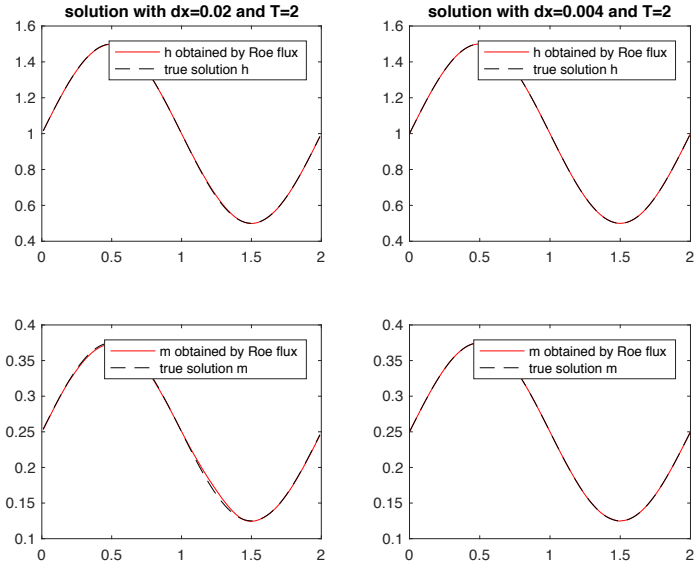

Figure 35: Numerical solution with minmod-type tvb limiter for M=64

4.2 second case

We repeat what we did in the previous subsection with periodic boundary conditions, zero as source term and the following initial conditions:

$$h(x,0) = 1 - 0.1sin(\pi x)$$

and

$$m(x,0) = 0.$$

As reference solution we compute once a solution with the MUSCL limiter on a very fine mesh ($\Delta x = 0.0005$).

Zero slope

We observe the numerical solution at final time $T = 2$ against the reference one for two different number of point grids (Figure 36).

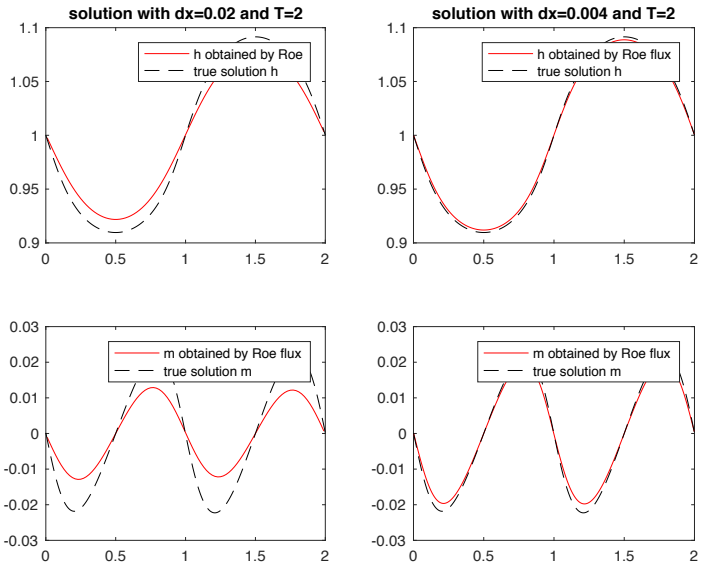

Figure 36: Numerical solution with zero slope

We plot also the error as function of Δx and we observe that the order of convergence is 1 (Figure 37).

Minmod limiter

We run the experiment with the Minmod limiter. In Figure 38 we can see the numerical solution against the true solution (the reference one).

The plot of the error at final time as function of Δx can be find in Figure 39. As expected the error decay is 2.

MUSCL limiter

In Figure 40 we find the numerical solution with muscl limiter against the reference one at final time.

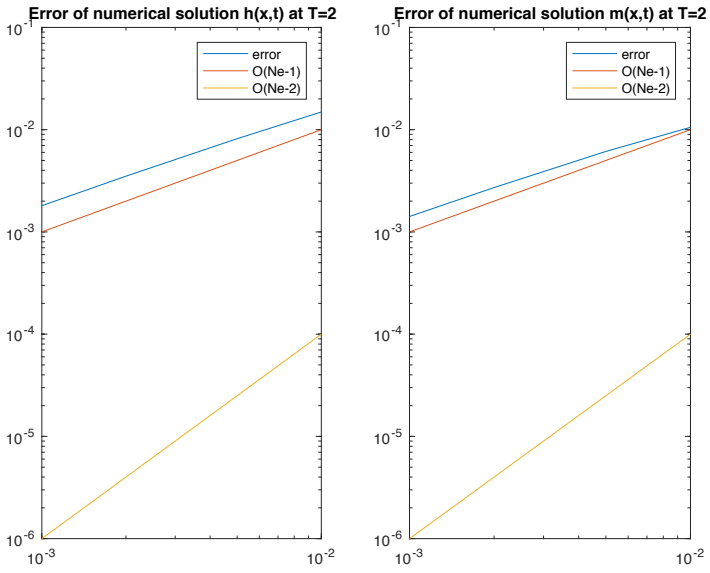

Figure 37: Numerical error with zero slope

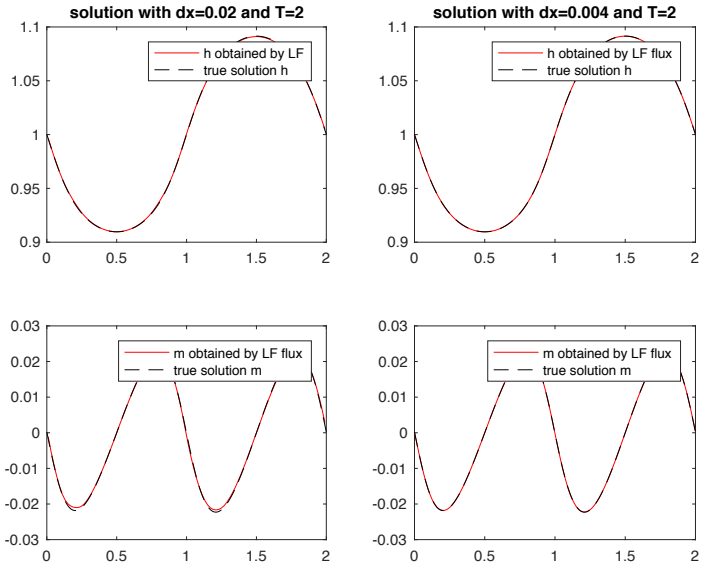

Figure 38: Numerical solution with minmod limiter

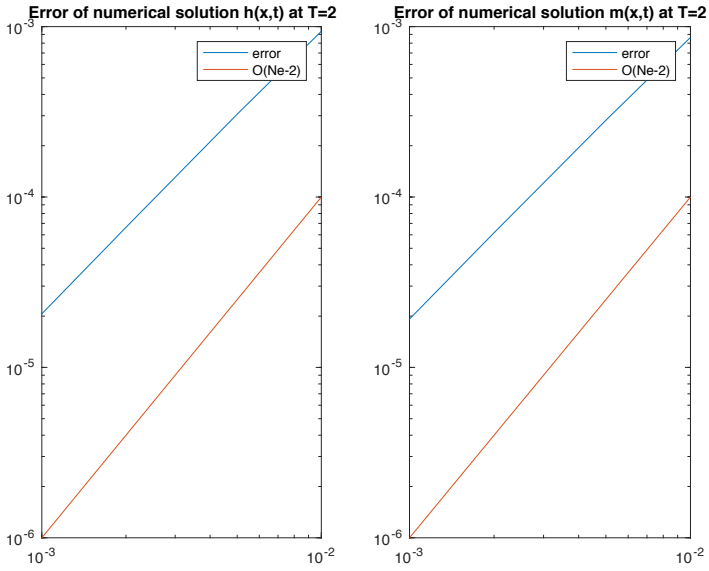

Figure 39: Numerical error with minmod limiter

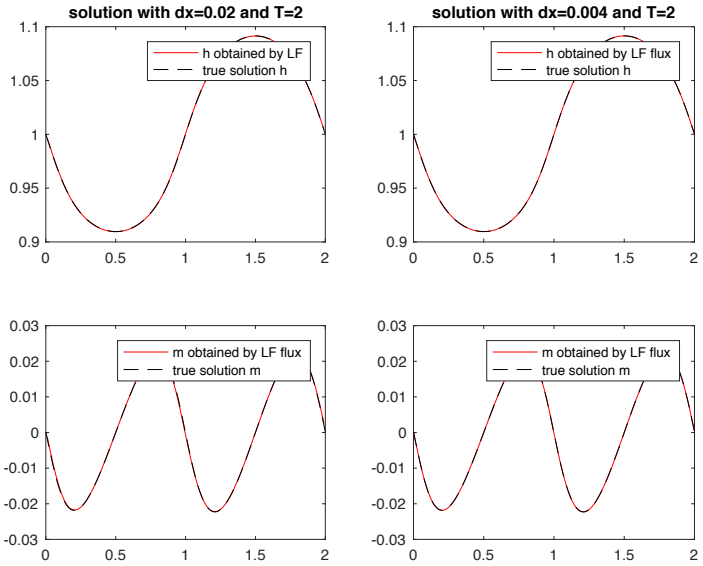

Figure 40: Numerical solution with muscl limiter

As always we also plot the error in a log-log graph and we observe an order of convergence in space of 2 (Figure 41).

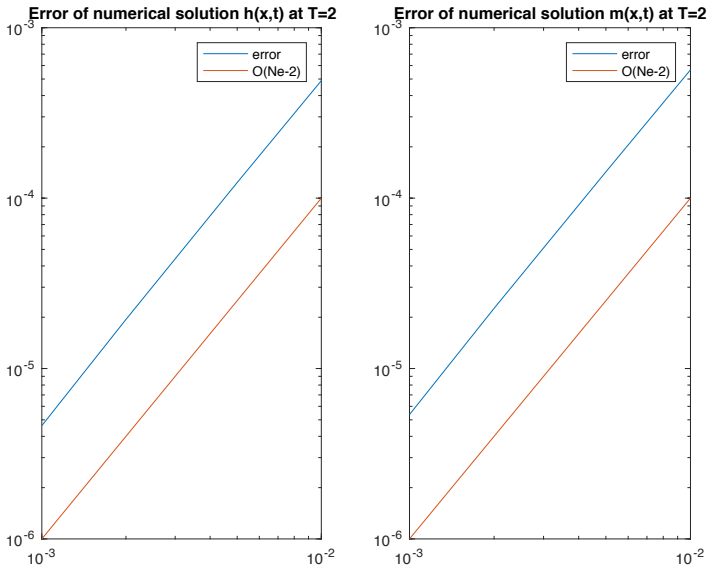

Figure 41: Numerical solution with muscl limiter

Minmod-type TVB limiter
We try to find M by looking at the smallest M that reach convergence rate 2. We choose $M = 80$ (Figure 42).
In Figure 43 we can observe the error at final time only for $M = 80$.
Last figure 44 shows the numerical solution at final time $T = 2$ for different number of grid points against a reference one.

4.3 third case

For this case we have zero source term, periodic boundary conditions and the following initial conditions:

$$h(x, 0) = 1 - 0.2sin(2\pi x)$$

and

$$m(x, 0) = 0.5.$$

As before we use a reference solution computed with the MUSCL scheme and a fine grid ($\Delta x = 0.005$). For all type of limiter the error looks similar to the case 3 of Lax-Friedrichs flux, because of the non derivability of the solution.
Zero slope
In Figure 45 we can observe the numerical solution at final time against the reference one.

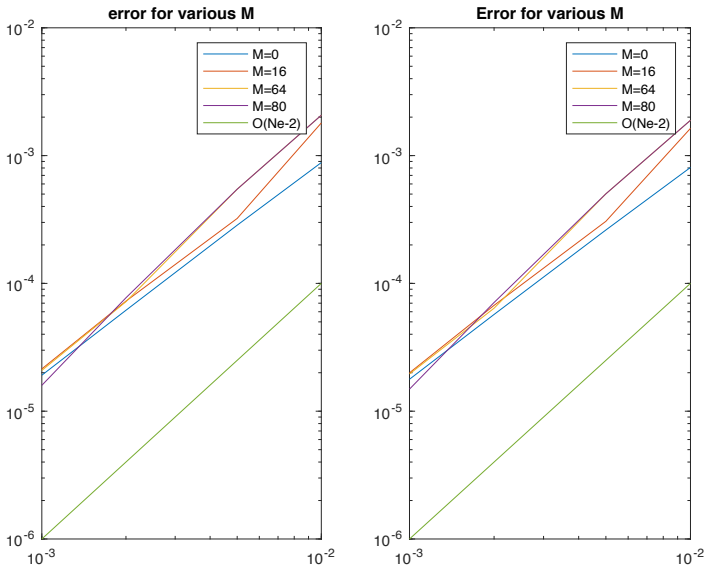

Figure 42: Numerical error for different M with minmod-type tvb limiter

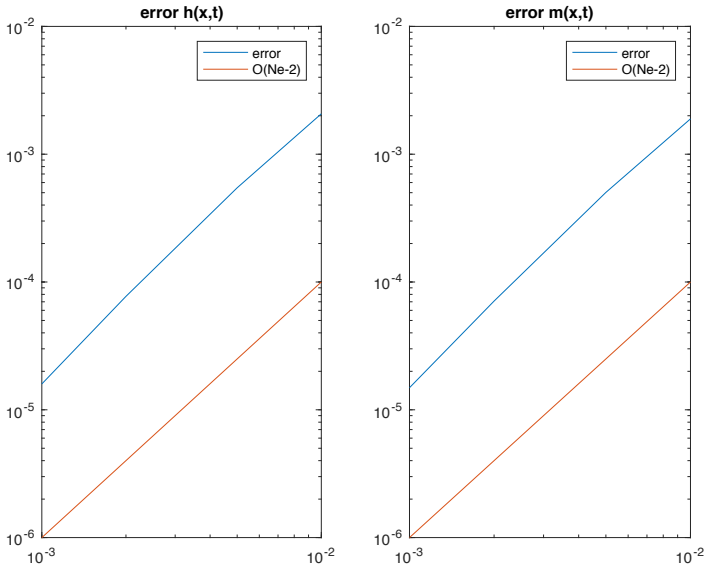

Figure 43: Numerical error with minmod-type tvb limiter and $M = 80$

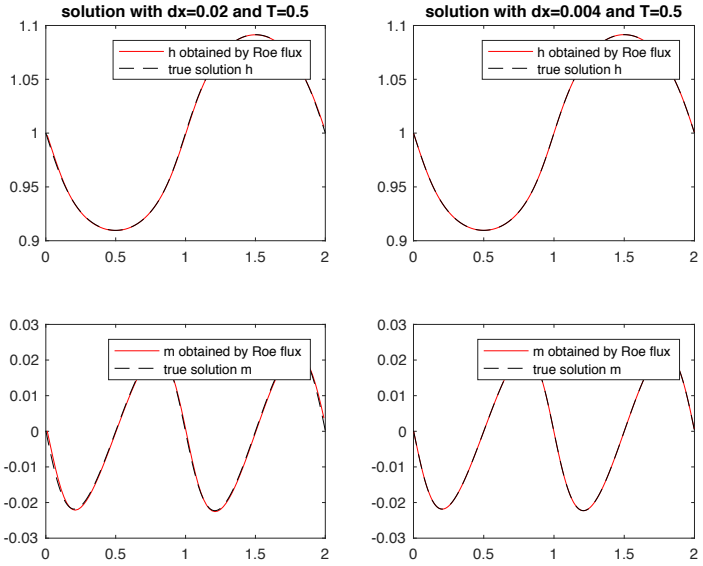

Figure 44: Numerical solution with minmod-type tvb limiter and $M = 80$

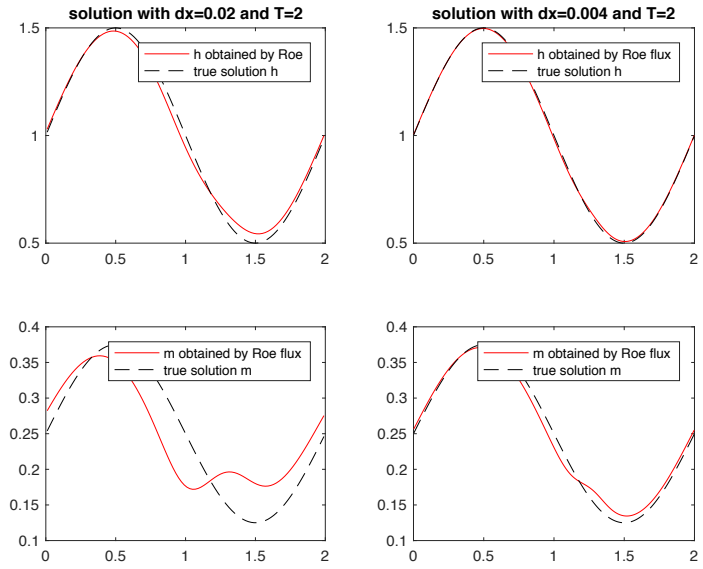

Figure 45: Numerical solution with zero slope

In Figure 46 we observe the numerical error at final time.

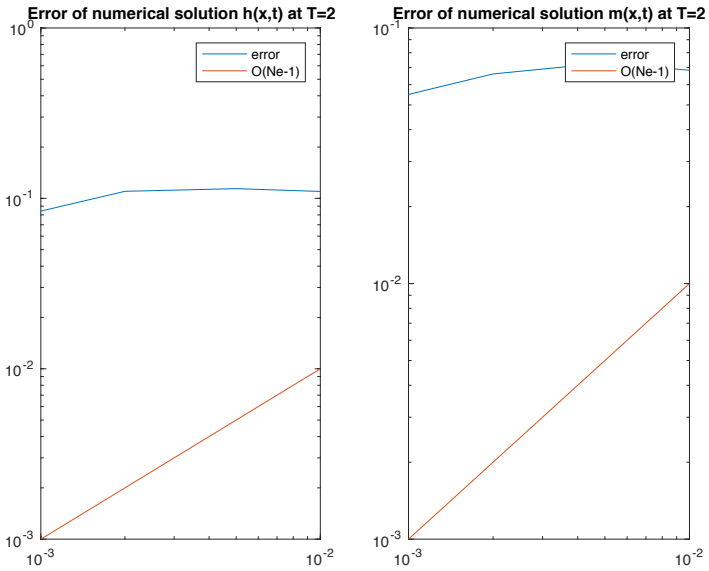

Figure 46: Numerical error with zero slope

Minmod limiter We plot the numerical solution at time $T = 2$ against the reference one with the minmod limiter (Figure 47).

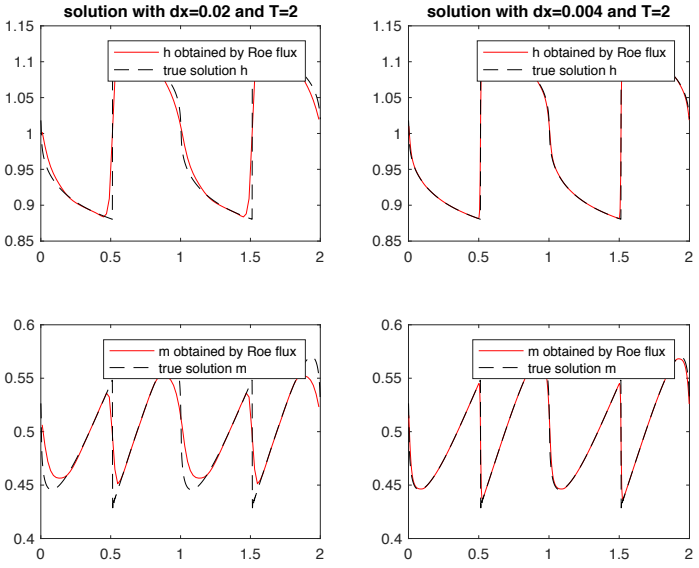

Figure 47: Numerical solution with minmod slope

Moreover in Figure 48 we can observe the numerical error at final time.

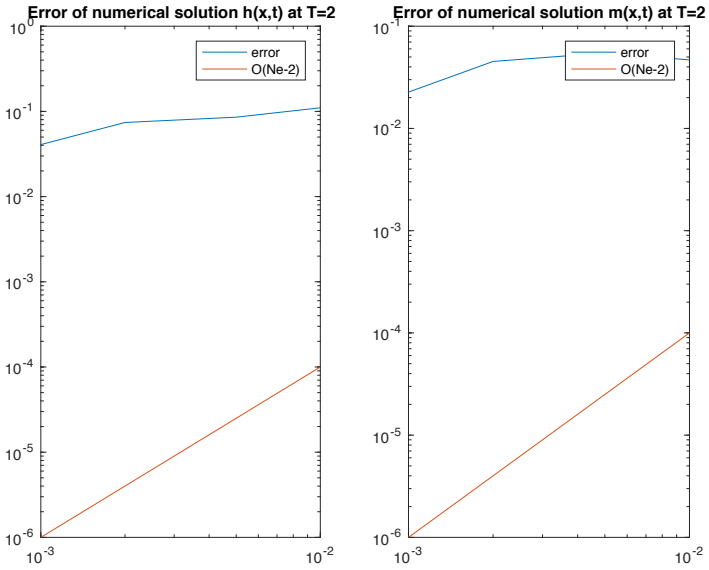

Figure 48: Numerical error with minmond slope

MUSCL limiter
In Figure 49 we observe the numerical solution at final time against the reference.

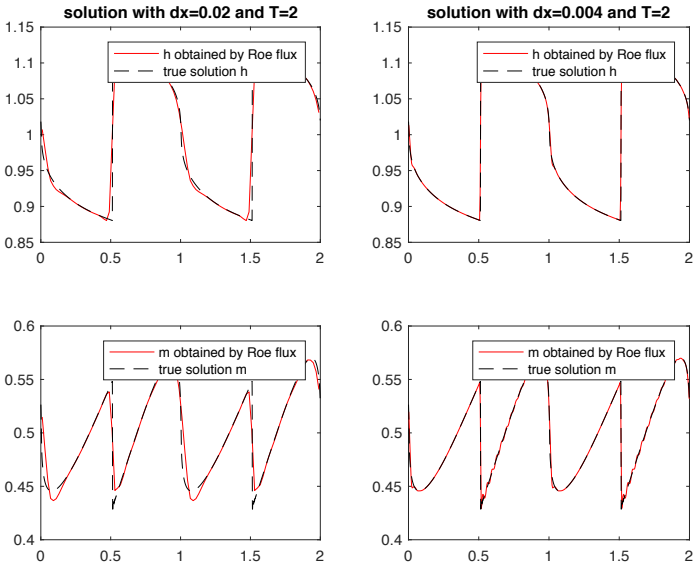

Figure 49: Numerical solution with muscl slope

We can observe again the measure of the error at final time as function of Δx (Figure

50).

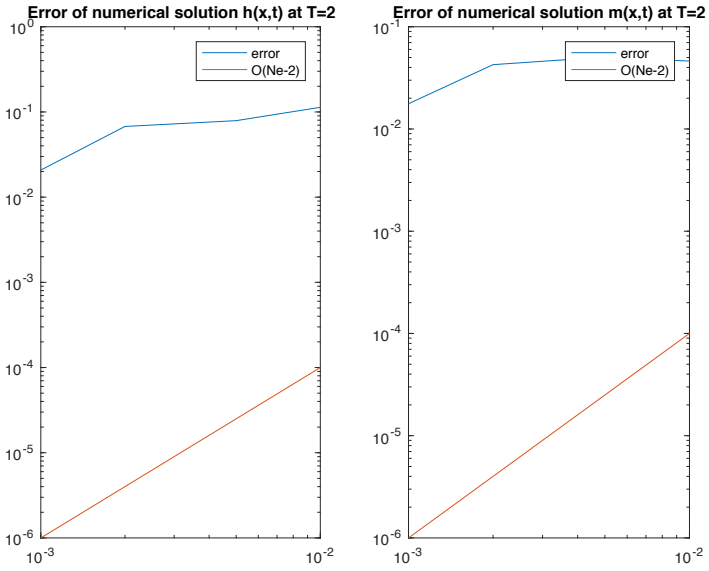

Figure 50: Numerical error with muscl limiter

Minimod-type TVB limiter
We try to use the biggest M that doesn't add oscillations. We choose $M = 5$, in fact already with $M = 10$ we have some small oscillations. So M is clearly not the same for all initial conditions, thus the choice of M clearly depends on the initial condition. We plot the numerical solution against the reference one at final time (Figure 51).
In Figure 52 we can observe the numerical error with $M = 5$.

4.4 Fourth case

We are now studying the one-dimensional shallow water equation with open boundary conditions, zero source term $S = 0$, with final time $T = 0.5$ and the following initial conditions:

$$h(x, 0) = 1$$

and

$$m(x, 0) = \begin{cases} -1.5 & \text{if } x < 1 \\ 0.0 & \text{if } x > 1 \end{cases}$$

We obtain a reference solution with a very fine grid mesh ($\Delta x = 0.005$) and the Lax-Friedrichs flux. We try to run our code with the Roe flux for all the different slope limiter in order to observe if the problem of entropy violation observed in the first

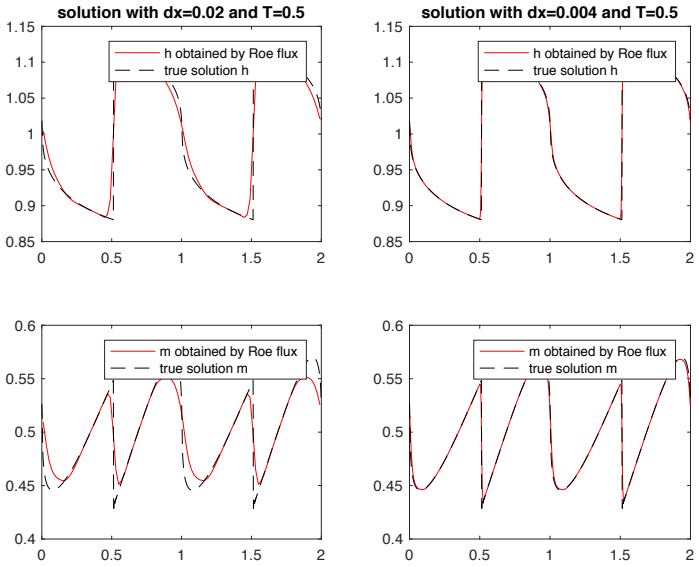

Figure 51: Numerical solution with minmod-type tvb limiter

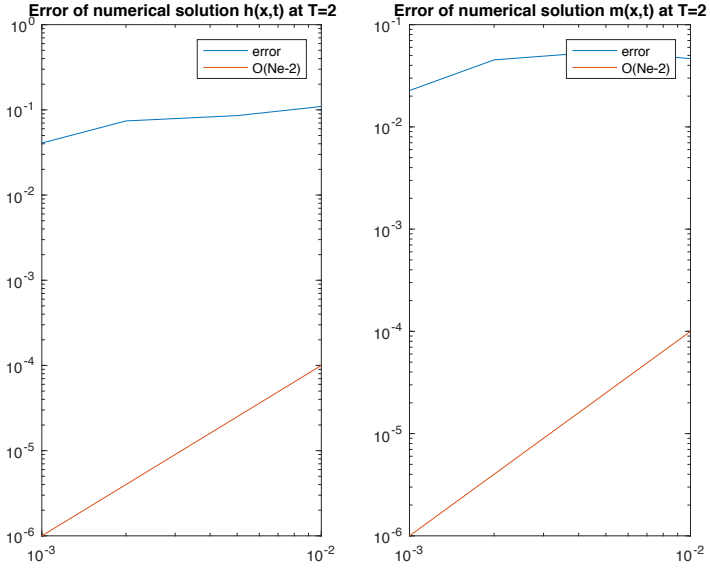

Figure 52: Numerical error with minmod-typ tvb limiter

project disappear with these approaches.
Zero slope
We observe the numerical solution at final time $T = 0.5$ against the reference one for two different number of point grids (Figure 53).

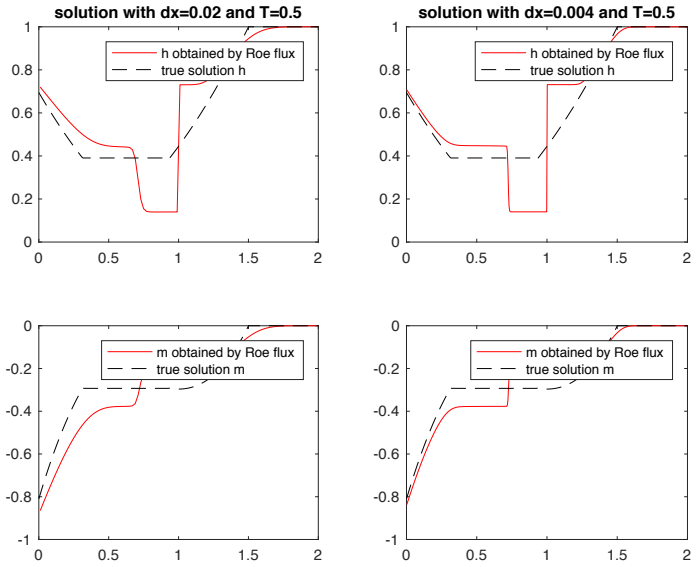

Figure 53: Numerical solution with zero slope

We notice that with zero slope (as expected) the entropy condition is still violated.
Minmod limiter
We run the experiment with the Minmod limiter. In Figure 54 we can see the numerical solution against the true solution (the reference one).
We observe that there are still some small oscillations, but this time works clearly better then with zero slope.
MUSCL limiter
In Figure 55 we find the numerical solution with muscl limiter against the reference one at final time.
Minmod-type TVB limiter
After some trials with different M we remark that approximately the bigger M we can use without reintroducing other oscillations is $M = 10$. For example with $M = 30$ we clearly can see other oscillations. So we plot the numerical solution at time $T = 0.5$ against the reference one (Figure 56).
So we observe that using a MUSCL approach with minmod, muscl and minmod-type tvb limiter the problem of entropy violation with Roe flux is in somehow contained althought if there are still small oscillations near to 1 for $h(x, t)$.

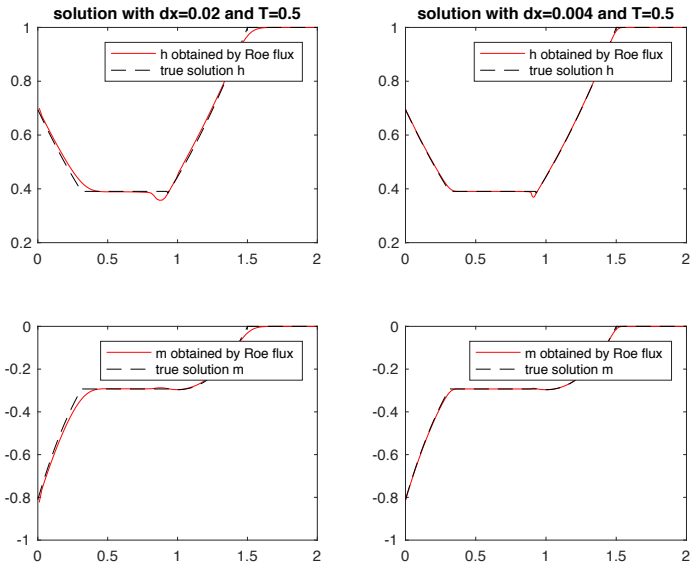

Figure 54: Numerical solution with minmod limiter

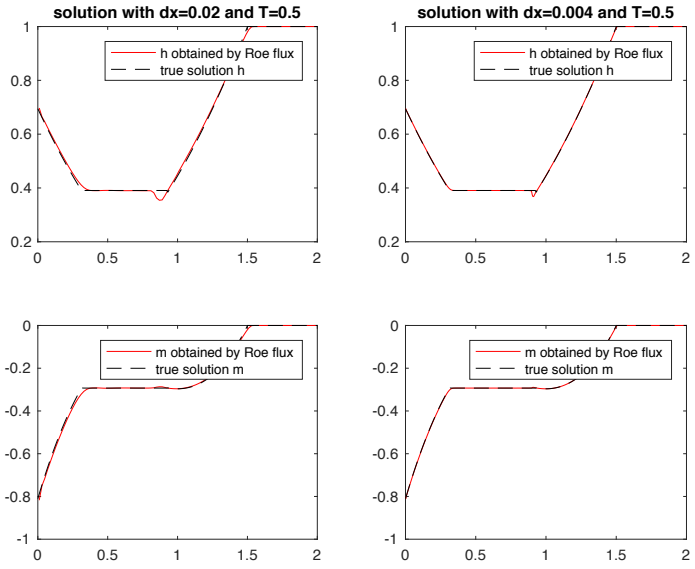

Figure 55: Numerical solution with muscl limiter

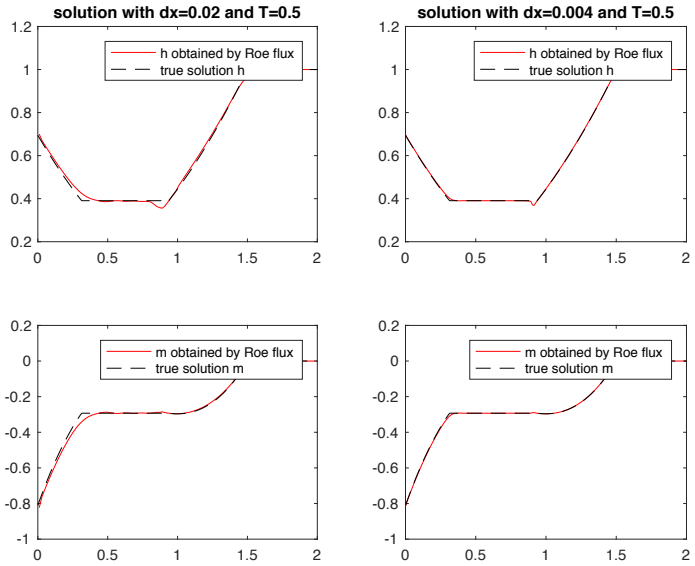

Figure 56: Numerical solution with minmod-type tvb limiter with $M = 10$